



Abdo, M., Toumpanaki, E., Diambra, A., Comandini, G., & Bank, L. (2023). *EVALUATION OF MECHANICAL PROPERTIES OF CONCRETE WITH RECYCLED FRP WIND BLADE WASTE MATERIAL*. Paper presented at 11th International Conference on Fiber-Reinforced Polymer (FRP) Composites in Civil Engineering, Rio De Janeiro, Brazil.

Peer reviewed version

[Link to publication record in Explore Bristol Research](#)  
PDF-document

## University of Bristol - Explore Bristol Research

### General rights

This document is made available in accordance with publisher policies. Please cite only the published version using the reference above. Full terms of use are available:  
<http://www.bristol.ac.uk/red/research-policy/pure/user-guides/ebr-terms/>

**EVALUATION OF MECHANICAL PROPERTIES OF CONCRETE WITH RECYCLED  
FRP WIND BLADE WASTE MATERIAL**

Meiran Abdo, University of Bristol, UK, meiran.abdo@bristol.ac.uk  
Eleni Toumpanaki, University of Bristol, UK, eleni.toumpanaki@bristol.ac.uk  
Andrea Diambra, University of Bristol, UK, andrea.Diambra@bristol.ac.uk  
Gianni Comandini, University of Bristol, UK, gianni.comandini@bristol.ac.uk  
Lawrence C. Bank, Georgia Institute of Technology, USA, lbank3@gatech.edu

**ABSTRACT**

The wider short-lived application of Fibre-Reinforced Polymer (FRP) composites especially in wind turbine blades raises questions about their end-of-life scenarios. A report by the National Composite Centre shows that nearly 14,000 wind turbine blades will be decommissioned globally which will generate nearly 50,000 tonnes of blades to be landfilled (NCC, 2022). Downcycling FRP materials in concrete applications is a promising and low energy intensive method for reducing the landfill amount. This study presents a new type of discrete reinforcing elements for concrete produced from waste FRP materials. FRP needles were derived from reclaimed wind blades made of GFRP and had a length of 50 mm and an aspect ratio of 36. FRP needles were incorporated in concrete to replace 2.5% of the coarse natural aggregate (NA) by volume. The concrete compressive and splitting tensile strength properties were compared to control specimens with 100% coarse natural aggregates. The results suggest that the incorporation of 2.5% FRP needles in concrete results in an increase in split tensile strength and only slight degradation in compressive strength.

**KEYWORDS**

Recycled Fibre Reinforced Polymers, Wind turbine blades, Concrete, and Experimental characterisation.

**INTRODUCTION**

Fibre-Reinforced Polymer (FRP) materials consist of a polymer matrix reinforced with carbon, aramid, or glass fibers. FRP composite materials are rapidly being used in various applications, including wind turbines, construction, sports equipment, and transportation, since they are lighter and possess excellent mechanical properties, corrosion resistance, a high strength-to-weight ratio, and moldability compared to traditional materials (Bank, 2006). The polymer resin can be classified as thermoplastic or thermosetting. Thermoplastic resins, such as polyurethane, polyvinyl chloride, or polyethylene, do not exhibit significant chemical changes during production, making it easy to convert them back to their initial monomer (Ageyeva et al., 2019). On the other hand, thermosetting resins, such as polyester and epoxy, undergo chemical changes during manufacturing, where their monomer chains form covalent bonds and a higher degree of cross-links. Therefore, thermosetting FRP materials are hard to recycle, unlike thermoplastic FRPs, which are easy to remelt (Pickering, 2006).

The global market for Fibre-Reinforced Polymer composites is rapidly growing and is estimated to reach 375 billion US dollars by 2026, with an annual growth rate of 7.3% (Qureshi, 2022). The transportation, wind energy, construction, and aerospace sectors are predicted to experience significant growth in the use of FRPs. However, this growth will also result in a larger amount of FRP waste. Managing and recycling FRP waste poses a challenge for industries, especially when it comes to thermosetting FRP composites, as the available waste management solutions are limited (Pickering, 2006).

In the wind energy sector, GFRP composites are primarily utilized in the production of wind turbine blades, offering advantages such as reduced weight and increased stiffness for larger and longer blades. In 2018, Europe installed nearly 77,000 wind turbines. Considering the relatively short service life of these turbines, which is approximately 20-25 years, a significant amount of FRP waste will be generated, most likely ending up in landfills or being incinerated in the near future (Jensen & Skelton, 2018). According to Brown et al. (2022), the UK alone is projected to produce around 75,000 tons of GFRP scrap and 6,200 tons of GFRP waste annually. This waste production is expected to increase by 10%. Currently, approximately 90% of the GFRP waste in the United Kingdom is sent to landfills (Osmani & Asokan, 2010). Bank et al. (2018) estimated that global wind turbine blade waste will reach nearly 43 million tons by 2025. This estimation is based on wind power projections from the Global Wind Energy Council (GWEC, 2016) and aligns with the findings of Liu & Barlow (2016).

The mechanical recycling of GFRP in concrete is a promising approach for processing wind turbine blade waste, where the GFRP can be used in concrete as an aggregate replacement and reinforcing element. Prior studies found that the concrete compressive strength decreases gradually with the increase of the GFRP filler-sized waste ratio (Correia et al., 2011). Similar results were found by Shahria et al. (2013) and Fox (2016) for FRP waste obtained from wind turbine blades and a geometry similar to aggregates. According to Yazdanbakhsh et al. (2016), the decrease in concrete compressive strength with the use of FRP waste is attributed to the FRP smooth surface which weakens the interfacial bonding between the cement and the FRP surface. The concrete mechanical properties with FRP needles are affected by interfacial bond conditions, shape, and resource of the FRP aggregates (Yazdanbakhsh et al., 2017).

Existing studies on concrete with FRP needles are limited, and the investigation of different shapes and replacement ratios of FRPs has not been thoroughly conducted. In this paper, FRP needles were obtained from reclaimed wind turbine blades made of GFRP. Each needle had a square cross-section measuring 6 mm by 6 mm and a length of 50 mm (with an aspect ratio of 36). These FRP needles were incorporated into the concrete mixture to replace 2.5% of the coarse natural aggregate (NA) by volume. Aggregate grading and surface analysis were considered to analyse the effect of surface roughness on the bonding between cement and FRPs. The failure patterns, split tensile strength, compressive strength, modulus of elasticity, and stress versus strain response were investigated. Future research stages will involve investigating different FRP replacement ratios and shapes of FRP needles.

## **EXPERIMENTAL PROGRAM**

### **Materials and Concrete Mixtures**

The needles used in this study were produced from reclaimed wind turbine blades provided by Vestas (Isle of Wight). The wind turbine blade's thickness ranged from 10 mm to 80 mm and was fully made of GFRP. The laminate consisted of 2 x Quasi-Isotropic +/- 45° layers followed by 9 x 0° layers. The fibre orientations were determined by undertaking several tests such as microscopy imaging and FRP burn-out test according to ASTM D2584 (ASTM, 2018). The materials, as provided by Vestas Technology R&D, are shown in Figure 1, and were resized to a smaller laminate for further processing at the University of Bristol concrete lab. In this study, the GFRP wind blades were cut down to needle shapes with a square cross-section of 60 mm x 60 mm and a length of 50 mm.



Figure 1: FRP wind turbine blade section before processing to FRP needles.

The data regarding the GFRP used to manufacture the blade was not made available to the research team. Therefore, a sequence of experiments has been conducted to confirm the fibre content, fibre direction of the GFRP and density (see Table 1). For ease of comparison with previous work on GFRP needles by Yazdanbakhsh et al. (2017), the produced needles in this study have similar cross-section but different needle length (50 mm) and aspect ratio (36), as depicted in Figure 2. The needles produced in Yazdanbakhsh et al. (2017) had a thickness of 6 mm and a length of 100 mm. In this study, shorter needles were investigated to approximate concrete micro-reinforcement due to their high stiffness and larger aspect ratio compared to the coarse aggregate. Moreover, a shorter needle will potentially benefit the flowability of the resulting concrete mix in a dense steel reinforcement cage in concrete structures. All the above-mentioned cutting processes were performed by using a table saw with a diamond blade.

Table 1: Properties of GFRP reclaimed wind blade.

Properties	Type (Value)
Fibre Content by Weight (%)	64
Density ( $\text{kg/m}^3$ )	1930-2070
Fibre type	E glass fibre*

Note: \*Most GFRP wind turbine blades are made of E-glass fibres (Eker et al., 2006).



Figure 2: FRP needles produced.

The aggregate used in this study (crushed Limestone) was graded with a hand sieve shaker to check that the size gradation complies with the ASTM C33 (ASTM, 2013) standards. ASTM-graded sand and Type I Portland cement were used in all concrete mixtures. Both aggregate and sand have been used in saturated surface-dry (SSD) conditions to ensure a constant water/cement ratio. The proportions of the concrete mixtures are presented in Table 2. Two types of specimens were produced: a control concrete specimen without FRP needles which is referred to as control-NA, and a concrete specimen with FRP needles 2.5% (by volume) as a replacement for coarse aggregate, which is referred to as FRP-RA-2.5. The FRP-RA-2.5 specimens were produced using the same material proportions (but aggregates) with the control specimens (control - NA). The target water-cement ratio of the concrete mix was 0.45. No adjustment for the overall mixed water was made due to the low moisture absorption of the FRP needles, as experimentally observed after 14 days with ongoing water absorption tests. Due to the size of the available mixer in the lab, two concrete batches were prepared. The first batch was used for control samples and the second batch was used for samples with FRP needles and 2.5% replacement ratio (by volume). Each batch produced 8 cylinders with a height of 300 mm and a diameter of 150 mm. Four specimens were used for splitting tensile strength tests and the remaining four specimens were used for compressive strength tests. In the compressive tests, the compressive modulus of elasticity was measured using two LVDTs mounted on each side of the concrete cylinder. After 24 hours the samples were de-moulded and put into a water curing tank for 14 days, where the temperature remained at  $20 \pm 2$  °C. A slump test was performed according to ASTM C143 (ASTM, 2015).

Table 2: Proportions of the concrete mixtures including the number of needles for 2.5% replacement.

	Mixture	
	Control- NA	FRP-RA-2.5
Cement	422	422
Sand (SSD)	683	683
Aggregate (SSD)	950	926
Water	190	190
FRP Needles	0	38
Slump (mm)	80	72

A sieve analysis was performed on the aggregates according to ASTM C33 (ASTM, 2018) standards to investigate the distribution of the particle sizes. The aggregate sizes ranged between 2.4 to 23 mm, as shown in Figure 3.

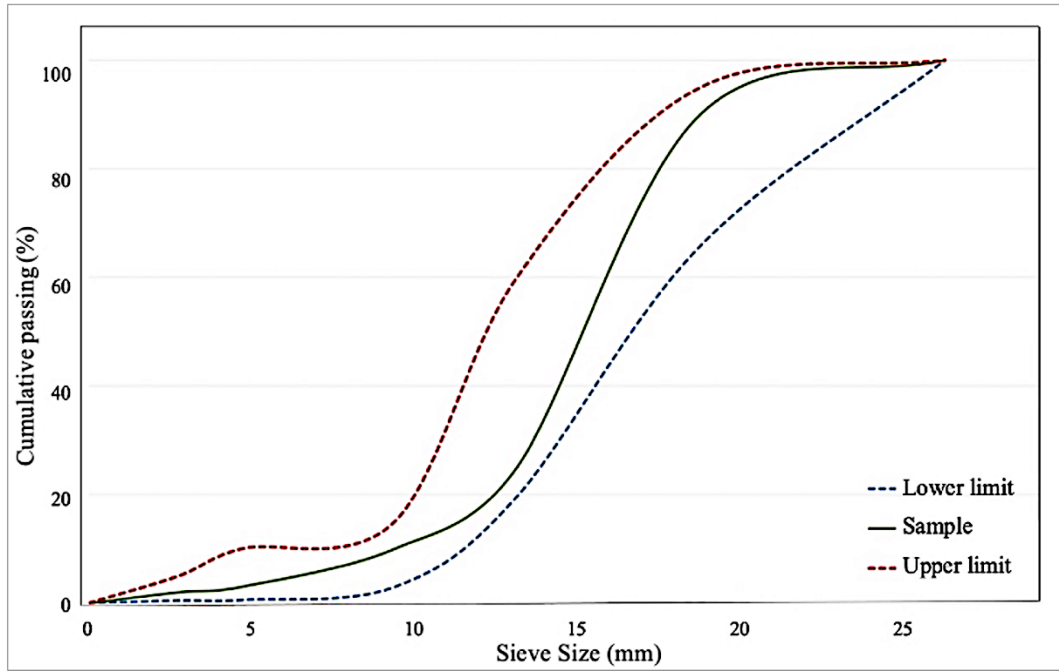


Figure 3: Grading curves of coarse aggregates showing the ASTM C33 (ASTM, 2018) lower and upper limits.

## TEST METHOD

Compressive and splitting tensile strength tests were conducted on both the control-NA and FRP-RA-2.5 specimens after 14 days of curing. The concrete compressive strength and the compressive modulus of elasticity were evaluated according to ASTM C469 (ASTM, 2014). The splitting tensile strength was conducted according to ASTM C496 (ASTM, 2011). The LVDT setup in the compressive tests was made at the University of Bristol, as shown in Figure 4a, with mounting of 2 LVDTs at each side of the concrete cylinder. The LVDTs were connected to a data logger to record the relative concrete contraction within the gauge length and calculate the concrete compressive modulus elasticity. The split tensile tests were conducted using the INSTRON 600DX Testwell machine with a maximum load capacity of 3000 KN. For measuring the strain during a split tensile test, a strain gauge is attached on the cross-section of the cylinders (centered), as shown in Figure 4b.

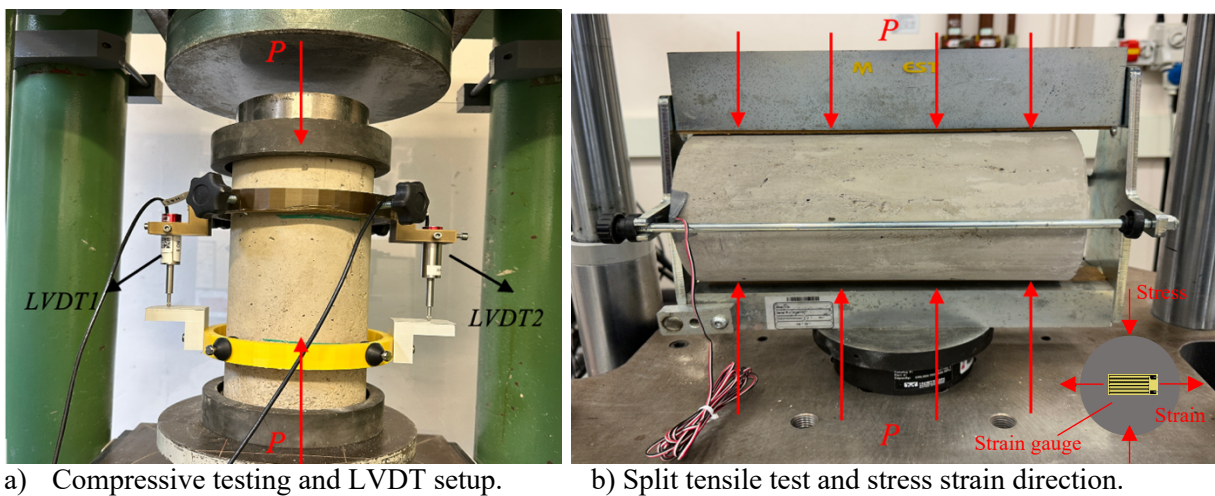


Figure 4: Mechanical characterisation of both control-NA and FRP-RA-2.5 concrete samples.

## NEEDLES SURFACE ANALYSIS

A surface analysis was conducted to determine the surface roughness of the FRP needles using an ALICONA imaging machine. To obtain the surface roughness measurements, nine FRP needles were used, including 3 sandblasted FRP needles (Figure 5b), and 3 glass blasted (Figure 5c) which have been compared to 3 needles with no blasting (smooth surface) (see Figure 5a). The results have shown a smooth surface was generated due to the diamond blade cutting for producing the small needles.

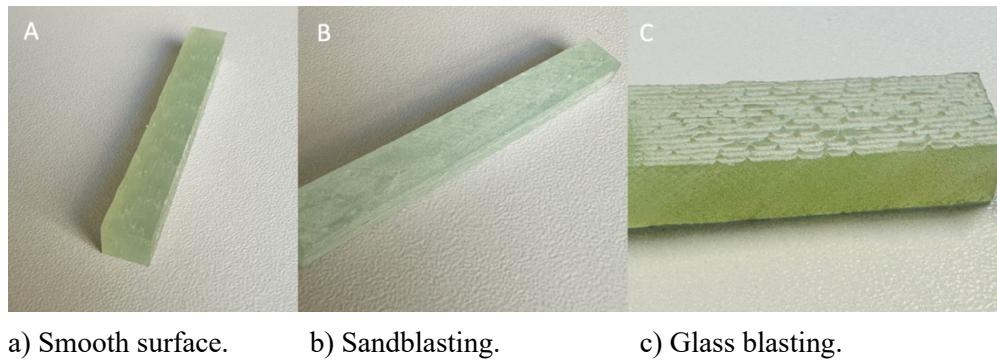


Figure 5: FRP needles surface roughness type.

To roughen the surface of the FRP needles, sandblasting (80 grid) and glass blasting (10 grid) were used. These techniques were expected to benefit the interfacial bonding between the needles and the mortar. Table 3 shows the average profile surface roughness ( $\mu\text{m}$ ) of three needles for each blasting method. It is worth mentioning that only sandblasted FRP needles were used here for the FRP-RA-2.5 samples and the rest blasting methods are investigated with bond tests for future use in FRP concrete.

Table 3: Surface analysis results of the different blasting methods.

Blasting Grid	Average profile surface roughness ( $\mu\text{m}$ )	Standard deviation, $\sigma$ ( $\mu\text{m}$ )	Profile Length (mm)
No blasting	6.176	0.147	50
Sand 80 grid	7.078	0.117	50
Glass 10 grid	19.703	0.214	50

The results show that sandblasting increased the surface roughness profile by only 7.1% compared to the FRP needles with no blasting. The glass blasting method will ultimately increase the FRP needle's surface roughness by 219.0%. This is an indication that glass blasting is more effective in terms of roughening the FRP needles. However, using glass blasting will cause more damage to the resin and glass fibre of the FRP needle's surface and this may in turn affect the durability of the FRP needles and the concrete mixture overall. There are many types of glass fibre, A, C, E, and S. The main difference comes in their chemical compositions. The commonly used glass fibre is E-glass for GFRP applications due to its low cost, excellent tensile strength, and low water absorption rate (Bulent et al., 2006). However, all glass fibres are influenced by alkaline environments due to the presence of silica in the glass fibres (Mounts, 2007). The durability of glass fibre was examined in a previous study where alkaline resistant AR-glass and E-glass were compared under identical concrete exposure at high temperatures. The results showed a higher strength reduction in E-glass fibres compared to AR-glass type (Coricciati et al., 2009). Therefore, it is essential to study the effect of long-term exposure to moisture and alkali environment of the embedded needles in later experiments with different needle replacement ratios.

## RESULTS AND DISCUSSION

### Slump flow

The number of FRP needles in the concrete samples with a 2.5% volumetric dosage is small resulting in slight differences in slump flow, as shown in Table 2. The observed deviations between concrete mixes are considered to be within experimental error. In general, the use of extra fibres reduces the slump flow measurements. The mix becomes more viscous. However, the needles are not small enough that can cause agglomeration (fibre agglomeration in fibre-reinforced concrete is common).

### Mechanical performance of concrete in compression

The compressive strength test results are presented in Table 4. The volumetric replacement of FRPs in concrete resulted in relatively small reductions in compressive strength. Replacing 2.5% of the aggregates in the control sample, by volume, with FRP needles reduced the concrete compressive strength from 39.9 to 36.9 MPa (reduction of 7.5%). A potential reason for the compressive strength reduction is that the aggregate crushed stones surface can have a better bonding in the concrete mixture compared with the FRP needles. However, the control samples failed suddenly when the compressive load achieved its peak value, while the FRP-RA-2.5 samples continue to carry some additional load which caused a less brittle failure compared with the control-NA samples (see stress and strain plot in Figure 6). The results agree well with Yazdanbakhsh et al. (2017) who showed that a 5% FRP volumetric replacement caused a slight reduction in compressive strength (by 6%) compared to the control samples.

Table 4: Compressive strength test results.

Concrete (GPa)	Specimen Type	$f_c$ (MPa)	$f_{cm}$ (MPa)	$f_{c\sigma}$ (MPa)	$E_c$ (GPa)	$E_{cm}$ (GPa)	$E_{c\sigma}$
Control NA	1	41.2	39.9	1.1	31.7	29.9	1.9
	2	38.9			28.6		
	3	39.3			27.7		
	4	40.1			31.3		
FRP-RA-2.5	1	37.5	36.9	0.9	26.2	26.4	0.7
	2	37.8			26.8		
	3	35.6			27.1		
	4	36.7			25.3		

Note:  $f_c$  = compressive strength,  $f_{cm}$  = average compressive strength,  $f_{c\sigma}$  = standard deviation in compressive strength,  $E_c$  = concrete elastic modulus,  $E_{cm}$  = average compressive elastic modulus and  $E_{c\sigma}$  = standard deviation in compressive modulus.

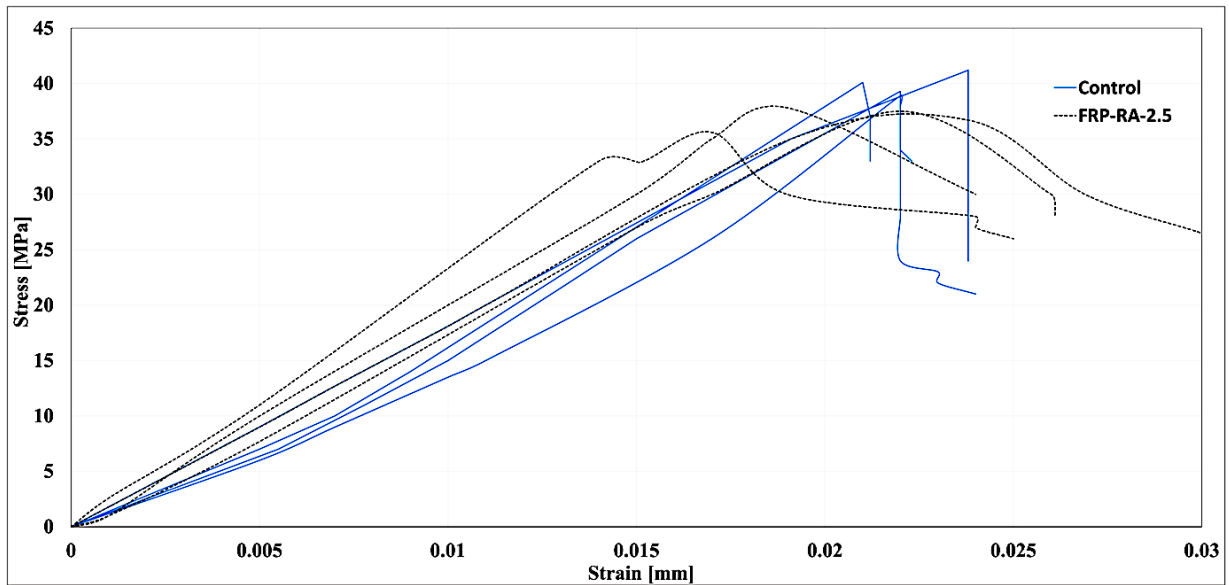


Figure 6: Stress-strain plots of concrete samples.

### Fracture patterns for compressive strength tests

All concrete sample fracture patterns were reported based on the ASTM C39 standards (ASTM, 2015b). Two major fracture patterns have been identified for the compressive strength tests of the concrete cylinder samples after 14 days of curing (see Figure 7). The most common failure pattern was a Type 1 well-formed cone on one end.



a) Failure pattern for control samples.

b) Failure pattern for FRP-RA-2.5 samples.

Figure 7: Samples of fracture patterns after the compressive test, (a) Control samples and (b) FRP-RA-2.5 samples.

### Mechanical performance of concrete in split tensile tests

The splitting tensile strength results are presented in Table 5. The FRP-RA-2.5 concrete samples yielded a 3.3 MPa average tensile strength which is 32 % higher than the respective value in the control samples. Yazdanbakhsh et al. (2017) reported a 13% reduction in concrete tensile strength when grooved needles are used at a 1.7% replacement ratio (by volume) and an aspect ratio of 17. Other work conducted by Yazdanbakhsh et al. (2017) reported a slightly similar splitting tensile strength.

Table 5: Split tensile strength test results.

Concrete	Specimen	$f_{ct}$ (MPa)	$f_{ctm}$ (MPa)	$f_{ct\sigma}$ (MPa)
Control-NA	5	2.8	2.6	0.1
	6	2.7		
	7	2.6		
	8	2.4		
FRP-RA-2.5	5	3.5	3.3	0.1
	6	3.1		
	7	3.4		
	8	3.3		

Note:  $f_{ct}$  = concrete tensile strength,  $f_{ctm}$  = average concrete tensile strength,  $f_{ct\sigma}$  = standard deviation of concrete tensile test results.

Figure 8 shows the tensile stress versus strain response of both control-NA and FRP-RA-2.5 samples. Post-peak tensile failure toughness was not observed in the FRP-RA-2.5 samples, despite the crack bridging effect in the failure modes.

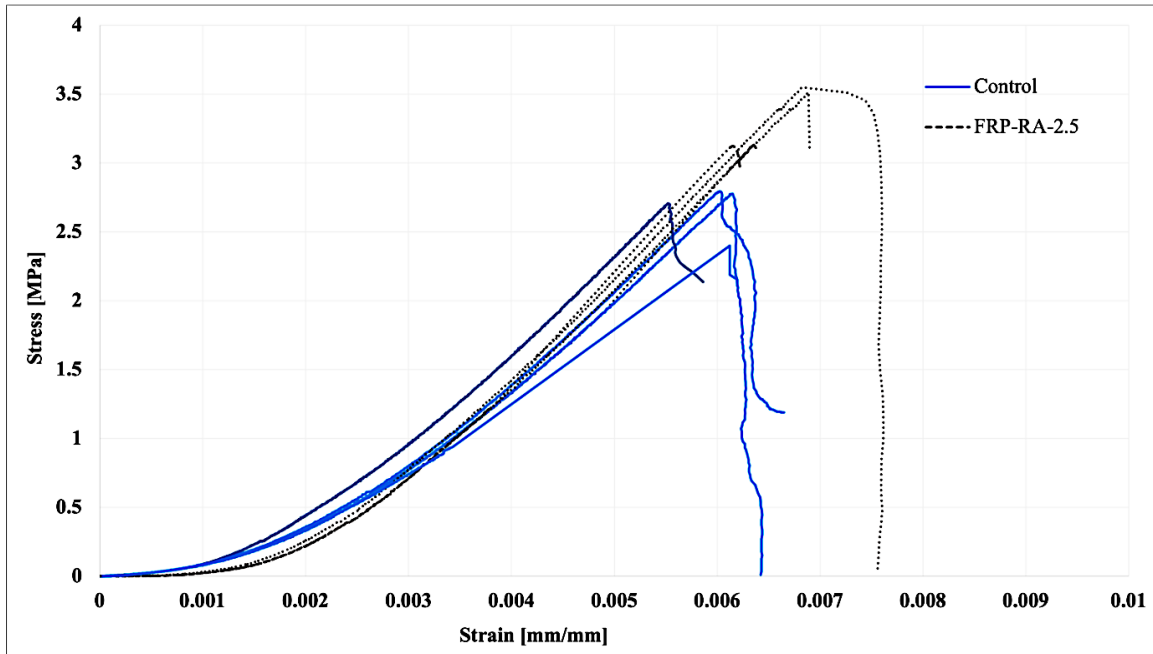


Figure 8: Splitting tensile stress versus strain.

#### Fracture patterns for concrete in split tensile tests

To examine the casting and curing of the concrete, all specimen fracture patterns were investigated according to the ASTM C39 standards (ASTM, 2015b). In the control samples, concrete cylinders were split into two pieces when the applied load reached the peak value (see Figure 9a). In the FRP-RA-2.5 concrete samples multiple cracks appeared, but the cylinder did not split open in two pieces after the peak failure load was attained (see Figure 9b). This indicates a beneficial crack-bridging effect with the FRP needles. After conducting the tests all cylinders were split open in two pieces for further analysis. It was observed that the FRP needles did not fail in tension and only pull-out bond failures were present (see Figure 10). The FRP needles were uniformly distributed.



a) Fracture patterns of control samples.



b) Fracture patterns of FRP-RA-2.5 samples.

Figure 9: Fracture patterns of split tensile tests.



Figure 10: Fractured surface of an FRP-RA-2.5 specimen.

## CONCLUSIONS

The landfill cost and the use of FRP materials is growing fast. FRP materials in civil engineering are not widely used, but there is a growing opportunity to solve the environmental impact of the FRP waste materials in the construction industry. Effective mechanical processing of waste materials and successful use in civil engineering applications with low structural demands (e.g., pavements) have been observed (RILEM, 2013). The addition of FRP needles obtained from wind turbine blade waste materials can enable the industry to allow more sustainable construction solutions.

This work presents the use of FRP needles with a small aspect ratio as an aggregate replacement or discrete reinforcement in concrete. Wind turbine blades do not have a consistent design approach; therefore, their material characterisation can be important for concrete practitioners in terms of durability and mechanical performance aspects. The results suggest the addition of FRP needles can have a significant positive effect on the split tensile strength with a slight reduction in the compressive strength. Surface bonding is a key element for improving the bond between the mortar and the FRP needles. Glass blasting methods can be the key to increase the bond performance.

Future developments in this research project include pull-out tests to study the bond strength of the FRP needles in concrete and use of the resulting data in FE models. The latter can shed light on the optimum geometry of the FRP needles and their effect on the concrete mechanical performance. A potential limitation is the effect of the FRP needle's size on the fresh concrete flowability in a vertical mould.

#### ACKNOWLEDGEMENT

- Vestas Technology R&D for providing the wind blade materials.
- Professor Valeska Ting University of Bristol who has acted as a great mentor.
- National Composites Centre NCC for providing technical support.

#### CONFLICT OF INTEREST

The authors declare that they have no conflicts of interest associated with the work presented in this paper.

#### DATA AVAILABILITY

Data on which this paper is based is available from the authors upon reasonable request.

#### REFERENCES

- Ageyeva, T., Sibikin, I., Kovács, J.G. A. (2019). Review of Thermoplastic Resin Transfer Molding: Process Modeling and Simulation. *Polymers*, 11, 1555. <https://doi.org/10.3390/polym11101555>
- ASTM. (2011). Standard test method for splitting tensile strength of cylindrical concrete specimens. ASTM C496, West Conshohocken, PA.
- ASTM. (2018). Standard Test Method for Ignition Loss of Cured Reinforced Resins, ASTM D2584, West Conshohocken, PA.
- ASTM. (2015b). Standard test method for compressive strength of cylindrical concrete specimens. ASTM C39, West Conshohocken, PA.
- ASTM. (2014). Standard Test Method for Sieve Analysis of Fine and Coarse Aggregates, ASTM C136, West Conshohocken, PA.
- ASTM. (2013). Standard specification for concrete aggregates. ASTM C33, West Conshohocken, PA.
- ASTM. (2014). Standard test method for static modulus of elasticity and Poisson's ratio of concrete in compression. ASTM C469, West Conshohocken, PA.
- ASTM. (2018). Standard Specification for Concrete Aggregates, ASTM C33, West Conshohocken, PA.
- Bank, L.C. (2006). *Composites for Construction: Structural Design with FRP Materials*. Wiley, Hoboken, NJ, USA.
- Bank, L. C., Arias, F. R., Yazdanbakhsh, A., Gentry, T. R., Al-Haddad, T., Chen, J.F., & Morrow, R. (2018). Concepts for reusing composite materials from decommissioned wind turbine blades in affordable housing. *Recycling*, 3(1). <https://doi.org/10.3390/recycling3010003>
- Brown, S., Forsyth, M., Job, S., Norton, A., Westaway, H., & Williams, C. (2020). *Renewables FRP Circular Economy Study: Industry Summary*. Retrieved from [https://compositesuk.co.uk/wp-content/uploads/2021/10/FRP-CE-Report-Final\\_0.pdf](https://compositesuk.co.uk/wp-content/uploads/2021/10/FRP-CE-Report-Final_0.pdf)

- Coricciati, A., Corvaglia, P., & Mosheyev, G. (2009). Durability of fibers in aggressive alkaline environment. ICCM International Conferences on Composite Materials.
- Correia, R., Almeida, N., & Figueira, J. (2011). Recycling of FRP composites: Reusing fine GFRP waste in concrete mixtures. *Journal of Cleaner Production*, 19(15), 1745–1753. doi: 10.1016/j.jclepro.2011.05.018.
- Eker, B., Akdogan, A., & Vardar, A. (2006). Using of Composite Material in Wind Turbine Blades. *Journal of Applied Sciences*, 6 (14), 2917-2921. DOI: [10.3923/jas.2006.2917.2921](https://doi.org/10.3923/jas.2006.2917.2921)
- Fox, T.R. (2016). Recycling Wind Turbine Blade Composite Material as Aggregate in Concrete. MSc Thesis. Iowa State University.
- Global Wind Energy Council. (2016). *Global Wind Report—Annual Market Update*. Global Wind Energy Council: Brussels, Belgium.
- Jensen, J.P., & Skelton, K. (2018). Wind turbine blade recycling: Experiences, challenges and possibilities in a circular economy. *Renewable and Sustainable Energy Reviews*, 97,165-176.
- Liu, P., & Barlow, C.Y. (2016). The environmental impact of wind turbine blades. *IOP Conference Series: Materials Science and Engineering*, 139(1), 012032. doi:10.1088/1757-899X/139/1/012032.
- Mounts, J. L. (2007). Durability of glass-fiber-reinforced polymer composites in an alkaline environment. MSc Thesis. West Virginia University. <https://researchrepository.wvu.edu/etd/1804>.
- NCC (National Composites Centre) (2022). *SusWIND Accelerating sustainable composite materials and technology for wind turbine blades*. Available at: <https://www.nccuk.com/what-we-do/sustainability/suswind/>.
- Osmani, M., & Asokan, P. (2010). An assessment of the compressive strength of glass reinforced plastic waste filled concrete for potential applications in construction. *Concrete Research Letters*, 1, 1-5.
- RILEM. (2013). Progress of Recycling in the Built Environment, Final Report of the RILEM Technical Committee 217-PRE, E. Vázquez, (Ed.), RILEM, Bagneux, FRANCE.
- Pickering, S.J. (2006). Recycling technologies for thermoset Composite materials – current status. *Composites Part A: Applied Science and Manufacturing*, 37(8), 1206-1215.
- Qureshi, J. A. (2022). Review of Recycling Methods for Fibre Reinforced Polymer Composites. *Sustainability*, 14, 16855. <https://doi.org/10.3390/su142416855>
- Shahria, A., Emma, S., Muntasir A. H. M. (2013). Green concrete made with RCA and FRP scrap aggregate: Fresh and hardened properties. *Journal of Materials in Civil Engineering*, 25(12), 1783-1794. doi:10.1061/(ASCE)MT.1943-5533.0000742.
- Yazdanbakhsh, A., Bank, L.C., Chen, C. (2016). Use of recycled FRP reinforcing bar in concrete as coarse aggregate and its impact on the mechanical properties of concrete. *Construction and Building Materials*, 121, 278-284. doi:<https://doi.org/10.1016/j.conbuildmat.2016.05.165>.
- Yazdanbakhsh, A., Bank, L.C., F., Chen, C., & Tian, Y. (2017). FRP-Needles as Discrete Reinforcement in Concrete, *Journal of Materials in Civil Engineering*, 29(10), 04017175. doi:10.1061/(ASCE)MT.1943-5533.0002033.